

Supplementary Materials

Reliable Preparation and Regeneration of Well-Defined Single-Atom Tips through Laser Annealing

Tzu-Chieh Yen¹, Wun-Cin Huang¹, Chun-Yueh Lin¹, Ming-Chang Chen^{2*}, Kung-
Hsuan Lin^{1*}, and Ing-Shouh Hwang^{1*}

¹Institute of Physics, Academia Sinica, Nankang, Taipei, Taiwan, R.O.C.

² Institute of Photonics Technologies, National Tsing Hua University, Hsinchu,
Taiwan, R.O.C.

*Corresponding author.

Email address: mingchang.chen@mx.nthu.edu.tw (M.-C. Chen).

linkh@sinica.edu.tw (K.-H. Lin)

ishwang@phys.sinica.edu.tw (I.-S. Hwang).

1. Supporting Note

2. Supporting Figures

Supporting Note

Determination of tip temperature during laser illumination

The temperature-dependent field emission current is well described in Fowler–Nordheim theory. The total current density emitted from a field emission tip is the sum of the products of the longitudinal velocities of the electrons and their transmission probability weighted using a carrier distribution function.

$$j_q(F, T) = \frac{q}{(2\pi)^3} \int \left(\frac{\hbar k_x}{m} \right) D(k_x, F) f(\vec{k}, T) d\vec{k} \quad \text{Eq. (1)}$$

In (1), q is the negative elementary charge, $D(k_x, F)$ is the transmission probability of electrons with longitudinal velocity $\frac{\hbar k_x}{m_e}$ as a function of local electric field strength F , \hbar is the reduced Planck constant, k_b is the Boltzmann constant, and $f(\vec{k}, T)$ is the Fermi–Dirac distribution at temperature T . To numerically solve integral function (1), the standard procedure is to integrate over transverse velocity components k_y and k_z under the assumption that the electrons are evenly distributed in velocity. Therefore, Eq. (1) can be simplified as follows:

$$j_q(F, T) = \frac{q}{2\pi\hbar} \int_0^\infty D(E_x, F) N(E_x, T) dE_x \quad \text{Eq. (2)}$$

where $N(E_x, T) = \frac{m_e k_b T}{\pi \hbar^2} \ln(1 + e^{(E_F - E_x)/k_b T})$ is the energy distribution of electrons, with E_x being the energy normal to the surface direction and E_F being the Fermi energy. Transmission probability $D(E_x, F)$ is governed by the potential barrier between the metal and vacuum level.

Potential energy for an electron inside the metal ($x < 0$) is considered flat and is referred to as 0 (Fig. S1). For an electron emitted from tip surface ($x > 0$), the potential barrier is

$$U(x) = \Phi + E_F - qFx - \frac{q^2}{16\pi\epsilon_0 x}$$

with Φ being the work function of the metal, the second term being Fermi level, the

third term being the potential variation due to electric field F , and the final term being image potential. Transmission probability $D(E_x, F)$ can be numerically calculated as follows through the Wentzel–Kramers–Brillouin (WKB) approximation:

$$D(E_x, F) = P(E_x) \exp\left[-\sqrt{\frac{8m_e q}{\hbar^2}} \int_{x_-}^{x_+} \sqrt{U(x) - E_x} dx\right]$$

, where x_- and x_+ are the classical turning points, and $P(E_x)$ varies slowly with energy and is approximated using constant $P(E_F) = \frac{4\sqrt{E_F \Phi}}{E_F + \Phi}$.

Given that $D(E_x, F)$ is a known function at field strength F , reconstructing normal energy distribution $N(E_x, T)$ from current density $J_q(F)$ with $J_q = \sigma j_q$ would be feasible; σ is a scaling factor that relates the measured electron count intensity to the theoretical current density j_q . As long as $N(E_x, T)$ is reconstructed, electron temperature T can be estimated.

We performed this reconstruction by discretizing Eq. (2) with respect to F and E_x (E for simplicity), which led to the following matrix equation:

$$J_q^{Fi} = \sum_{E_j} D^{FiE_j} N^{E_j}$$

Then, the linear inverse problem was solved with the least-squares method by minimizing the l_2 norm.

$$\arg \min \frac{1}{2} \left\| J_q^{Fi} - \sum_{E_j} D^{FiE_j} N^{E_j} \right\|_2^2 \quad \text{Eq. (3)}$$

For simplicity, we took $D^{FiE_j} = 1, \forall E_j > E_F + \Phi_{\text{eff}} = E_f + \Phi - \sqrt{\frac{q^2 F}{4\pi\epsilon_0}}$ because the transmission probability should equal the unity when energy surpasses the barrier height.

However, scaling factor σ and field enhancement factor β , which relates applied negative bias V to a tip's local electric field strength F through $F = \beta \frac{V}{r}$ (with r being the curvature radius of the tip apex), should be determined at the

beginning. The scaling factor accounts for the local emission area and microchannel plate (MCP) detection efficiency, whereas the field enhancement factor depends on the geometry of the tip apex; both are difficult to quantify through our experimental setup. To determine these factors, we first measured DC current versus tip voltage without laser illumination ($T_{RT} = 300$ K) and performed least-squares fitting to determine the free parameters. For fitting, we used $E_F = 6.06$ eV, estimated from the free-electron model, and $\Phi = 5.7$ eV for the Ir (111) surface.^{1,2} Our data were best fitted to $\sigma = 8.55$ nm² · s² and $\beta = 7.3$. These parameters were then used to estimate the temperature of the tip under laser illumination by fitting the relation of the DC current versus tip voltage under various laser powers.

Reference

1. J. C. Riviere, "Work function: Measurements and results," in Solid State Surface Science, edited by M. Green (Dekker, New York, 1969)
2. H. B. Michaelson, J. Appl. Phys. 48, 4729 (1977).

Supporting Figures

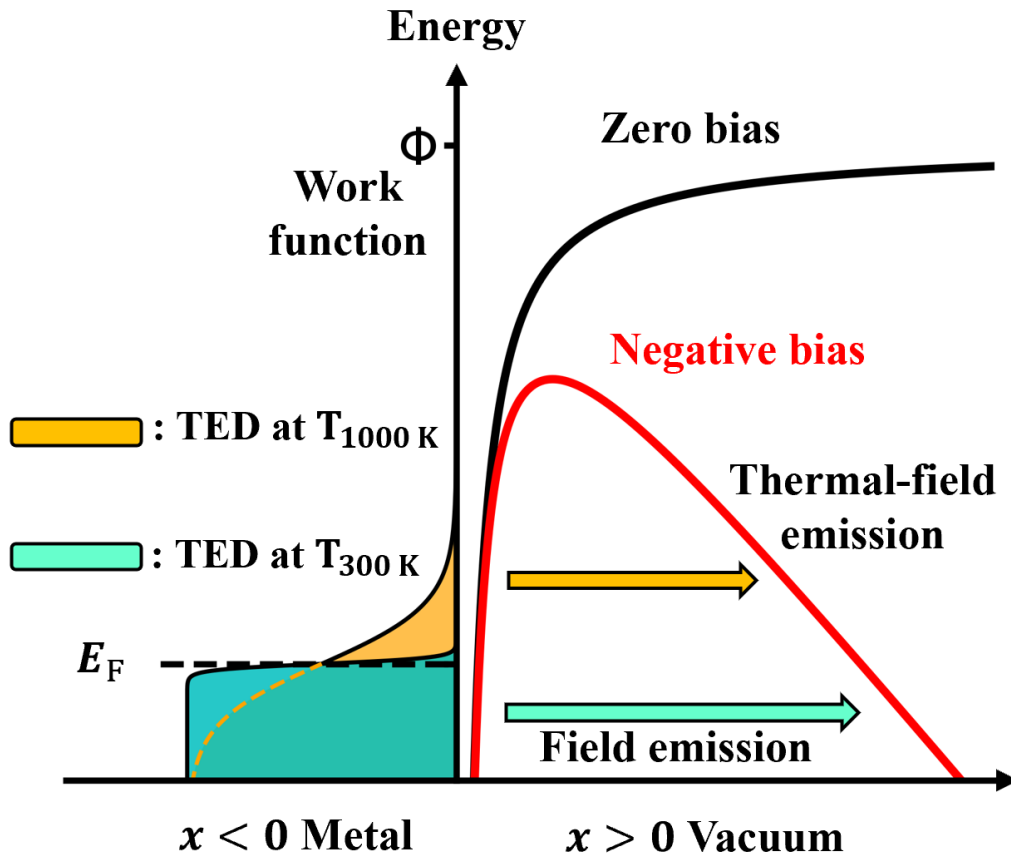


Fig. S1 Thermal-field emission model. TED denotes the total-energy distribution of the electron gas.

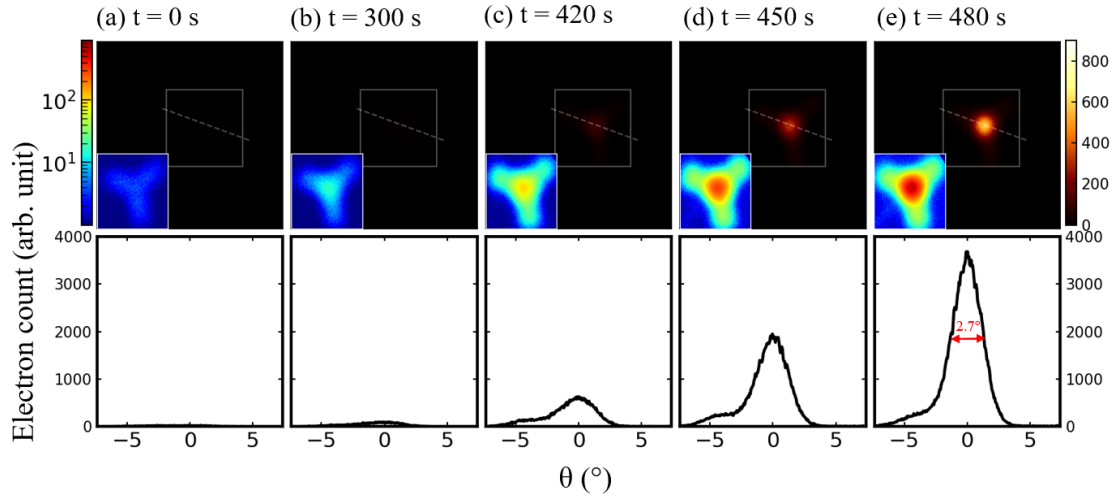


Fig. S2 Regeneration process of Ir-covered W(111) SAT through laser annealing in UHV. Top row: evolution of FE patterns during laser heating process over time. The color scale for all FE patterns is displayed on the right. The FE pattern was recorded at a tip bias of -900 V. A femtosecond laser beam (110 fs, repetition rate 50 MHz; 510 nm; 150 mw, polarized parallel to the axis of the tip shank) was used for heating. Insets: The FE patterns outlined in the white box are replotted on a log-intensity scale. Bottom row: corresponding intensity (linear) profiles along the white solid line on the top row.

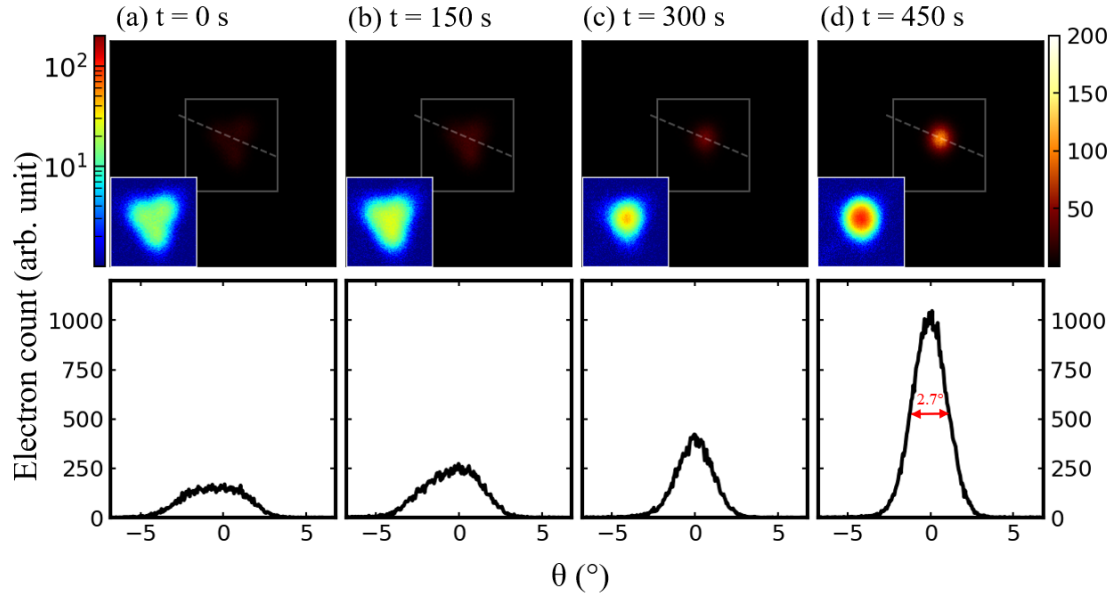


Fig. S3 Regeneration of a Au-covered W(111) SAT through laser annealing in UHV. Top row: evolution of FE patterns during laser heating process over time. The color scale for all FE patterns is displayed on the right. The FE pattern was recorded at a tip bias of -650 V. A CW laser beam (532 nm, 150 mw, polarized perpendicular to the long axis of the emitter) was used for heating. Insets: The FE patterns outlined in the white box are replotted on a log-intensity scale. Bottom row: corresponding intensity (linear) profiles along the white solid line on the top row.